ANALYSIS OF CLIMATE EFFECTS ON AGRICULTURAL SYSTEMS

DRAFT

A Report From:
California Climate Change Center

Prepared By:
Andrew Paul Gutierrez, Luigi Ponti, C.K. Ellis and Thibaud d'Oultremont
University of California, Berkeley

Arnold Schwarzenegger, *Governor*

WHITE PAPER

December 2005
CEC-500-2005-188-SD

Acknowledgements

Preface

The Public Interest Energy Research (PIER) Program supports public interest energy research and development that will help improve the quality of life in California by bringing environmentally safe, affordable, and reliable energy services and products to the marketplace.

The PIER Program, managed by the California Energy Commission (Energy Commission), annually awards up to $62 million to conduct the most promising public interest energy research by partnering with Research, Development, and Demonstration (RD&D) organizations, including individuals, businesses, utilities, and public or private research institutions.

PIER funding efforts are focused on the following RD&D program areas:

- Buildings End-Use Energy Efficiency
- Energy-Related Environmental Research
- Energy Systems Integration
- Environmentally Preferred Advanced Generation
- Industrial/Agricultural/Water End-Use Energy Efficiency
- Renewable Energy Technologies

The California Climate Change Center (CCCC) is sponsored by the PIER program and coordinated by its Energy-Related Environmental Research area. The Center is managed by the California Energy Commission, Scripps Institution of Oceanography at the University of California at San Diego, and the University of California at Berkeley. The Scripps Institution of Oceanography conducts and administers research on climate change detection, analysis, and modeling; and the University of California at Berkeley conducts and administers research on economic analyses and policy issues. The Center also supports the Global Climate Change Grant Program, which offers competitive solicitations for climate research.

The California Climate Change Center Report Series details ongoing Center-sponsored research. As interim project results, these reports receive minimal editing, and the information contained in these reports may change; authors should be contacted for the most recent project results. By providing ready access to this timely research, the Center seeks to inform the public and expand dissemination of climate change information; thereby leveraging collaborative efforts and increasing the benefits of this research to California's citizens, environment, and economy.

For more information on the PIER Program, please visit the Energy Commission's website www.energy.ca.gov/pier/ or contact the Energy Commission at (916) 654-5164.

Table of Contents

List of Figures

Abstract

- Species of plants and animals have specific requirement for growth, survival and reproductions that determine their geographic distribution, abundance, and interactions with other species.

- Commonly used growth indices and more recently developed weather driven physiologically based demographic models are reviewed and applied.

- The effects of climate warming on species dominance in alfalfa, pest range extension of pink bollworm in cotton, bloom dates and yield in olive, and the biological control of invasive vine mealybug in grape and the noxious weed yellow starthistle are examined using physiologically based models across the varied ecological zones of California. Geographic information systems (GIS) technology is used to map the effects of weather on plant/pest interactions across California.

- The models predict that the geographic range of the different species components of each system would be differentially affected complicating pest control issues. For example, pests such as pink bollworm on cotton would increase their range into formerly inhospitable areas, and their damage potential would increase in its current range. Similar predictions would also apply for other well-known pests such as Mediterranean fruit fly, olive fly and others. Changes in favorableness for some pests (for example, a weed such as yellow starthistle) would be more difficult to predict because of the effects on its natural enemies.

- The cultivation of annual crops could easily be moved to new areas as regional favorableness changes, while the reestablishment of long-lived species (e.g., grape and olive) would be costly to relocate in terms of time and money.

- The need to expand weather-gathering data systems and the development of physiologically based systems models of major cropping systems to forecast the dynamics of extant and new exotic pest introductions are identified.

1.0   Introduction

Pests are organisms of any taxa (e.g., arthropods, fungi, plants, vertebrates) that cause annoyance, disease, discomfort, or economic loss to humans. Most of our pests are exotic invasive species that, given current estimates, cause in excess of 137 billions of dollars in economic losses in the United States annually (Pimentel et al. 2000). Losses in California are likely in the range of 25-40 billion annually. In an ecological context, pests are merely filling evolved roles in ecosystems that may have been simplified, or disrupted through domestication, inputs of nutrients and toxic substances (pesticides), or by human mismanagement. In courts of law, pest outbreaks are often assumed to be acts of God, but considerable research has shown that pest outbreaks have important have climatic bases that affect their geographic distribution and severity.

Climate has profound impacts on the dynamics of agricultural and natural (e.g., fisheries and forestry) ecosystems, and yet the regulation at low levels of most species that feed on plants occurs largely unnoticed by humans (DeBach et al. 1964). But this delicate balance can be disrupted by climate change, and among the pioneering works were those of P.S. Messenger (1964, 1968). In their edited volume, Reddy and Hodges (2001) review many aspects of current thinking on the effects of climate change in agriculture. To examine the impact of climate change on these systems requires a holistic approach, often using models of the biology and dynamics of interacting as driven by weather and other factors. These models help explain how the species respond to extant weather; understanding that can then be extrapolated to examine the potential effects of climate change on their dynamics. Questions we might wish to examine are: (1) how climate change will affect the geographic range, phenology, survival, productivity, and damage by pests of economically important species in natural and managed systems, and (2) how natural and biological control systems that keep them in check will be affected. Unfortunately, the literature on field applications of these topics is sparse (see Gutierrez 2001).

1.1.   Review of Relevant Biological Modeling Literature

In the 19th and 20th centuries, time series plots of daily, weekly or monthly temperature, rainfall, vapor-pressure deficit, and other variables were used to create graphs that characterized climate zones favorable to plant and animal species. This empirical approach did not include the physiological growth response of species to climatic factors.

An important innovation was to characterizing the growth rates of species in response to abiotic variables including aspects of weather (Fritzpatrick and Nix 1968). For example, the normalized concave (i.e., humped) growth rate index of a species on temperature would predictably have lower and upper thresholds and an optimum for development. Similar functions could be developed for other abiotic variables such as moisture (i.e., vapor pressure deficit), soil PH and nutrient content and other factors. Any of these factors may greatly influence the distribution and abundance of species and the combined effects can be summarized mathematically. For example, the overall favorableness of conditions for growth (*GI*), say to temperature (*TI*), nitrogen (*NI*), soil water (*WI*), and other factors times t at coordinate location i,j is the product of the individual indices, each of which have values between 0 and 1 (eqn. 1).

$$0 \le GI_{ij}(t) = TI_{ij}(t)xNI_{ij}(t)xWI_{ij}(t)... \le 1 \tag{1}$$

A location becomes increasingly marginal as $G_{ij}(t) \to 0$, and any factor may make the site unfavorable because of the compounding effects. The growth index approach is an application of two old ideas, namely *von Liebig's Law of the Minimum* (1840) and *Shelford's Law of the Minimum* (1931). This study focuses on the effects of temperature and in some cases soil moisture.

Field data on the limits of favorableness to temperature directly and indirectly plant soil moisture of three common aphid pests. The bi-variate normal distributions of the data illustrated in **Figure 1** plots the average temperature (*TI*) and moisture (*MI*) indices during periods when aphid abundance was high (Gutierrez et al. 1974). Note that oat-apple aphid (*Rhopalosiphum padi*) thrives in cooler, wetter climes than, for example, the cowpea aphid (*Aphis craccivora*), which thrives in intermediate range of conditions, or the corn aphid (*R. maidis*), which thrives in hot, drier conditions. In general, each species in an ecosystem has its own set of unique conditions for growth and development. The most favorable conditions for the species would be in the central part of the bi-variate distribution and decrease towards the margins.
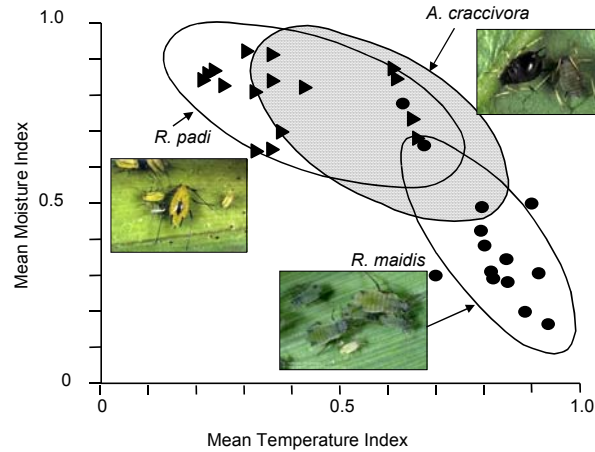
Figure 1. Bi-variate normal fits to indices of moisture and temperature of three exotic aphid pests (cf. Gutierrez et al. 1974; see also Sutherst et al. 1991).

In agriculture, agronomists through experimentation determine areas where specific crops grows best, but climate change could invalidate this knowledge. For example, the tolerance indices to temperature (*TI*) and moisture (*MI*) for the interaction of three hypothetical species (i.e., a plant, its pest, and its natural enemy) are shown in **Figure 2a**. (Note that these limits do not change except on an evolutionary time scale.) The dashed line in the figure is the average yearly pattern of *TI* and *MI* starting 1 January (i.e., the dot). The scenario in **Figure 2a** suggests a very good match of climate for the crop, while **Figure 2b** suggest moderate matching with increasing fall-winter-spring temperatures. **Figure 2c** depicts the effect of a large increase in rainfall. Such changes could readily occur due to climate change say in California. The plant has a broad response to temperature and moisture levels; that of the herbivore is intermediate, and that of the

predator is narrow. However, while the tolerances of three species remain unchanged (say **Figure 2a**), climate change could make the area more unfavorable (e.g., **Figure 2b-c**) or possibly more favorable. In reality, we are dealing with food webs that present a more complex problem, as illustrated in some analyses of field problems discussed below.

The importance of temperature on the regulation of pest was demonstrated using the case of the highly successful biological control of cottony cushion scale in citrus by the vedalia beetle (*Rodolia cardinalis*) and a parasitic fly (*Cryptochaetum iceryae*) (Quesada and DeBach 1973). (This biological control program has yielded hundreds of millions of dollars in benefit since 1887-1888 when the program was begun.) The biology of the parasitic fly restricts its range to cooler frost-free areas of California, while the vedalia beetle was able to control cottony cushion scale in hotter areas of citrus production (Quesada and DeBach 1973). In an other case, DeBach and Sundby (1963) showed that successive introductions of parasitoids to control California red scale on citrus resulted in a sequence of climatically better-adapted parasitoid displacing others in some areas. This displacement occurred until each species established in the subset of Californian environments most favorable for its development. These and other biological control successes could be jeopardized by climate change.
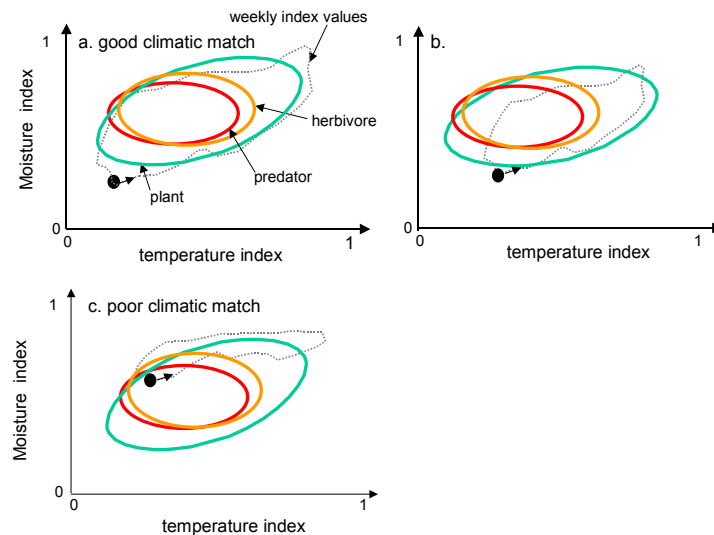
Figure 2. Climatic matching scenarios: (a) good, (b) moderate, and (c) poor. The yearly run of MI and TI values are depicted as the dashed line stating 1 January (i.e., ●).

1.2.   Physiologically Based Dynamic Modeling

To understand the dynamics of interacting species we must model the processes of growth, development, reproduction, and behavior of the species as driven by weather and other species in a general way—the model must be independent of time and place. Physiologically based demographic models of species have been developed that capture these processes (e.g., Gutierrez 1992, 1996; Gutierrez et al. 1975, 2005) and have early

roots in the pioneering plant physiology modeling work of Wit de and Goudriaan (1978). The models may include important aspects of the biology such as the capacity of some species to enter dormancy during periods of extreme temperature and/or moisture stress. Dormancy can have a strong influence on the yearly phenology of plant and animal species (e.g., Nechols et al. 1998), and even determine whether a species can survive in an area. These models capture these and other aspects of the biology and make predictions about the biological systems across the weather and ecological conditions of large landscapes such as California; prediction that can be mapped using geographic information systems (GIS) technology. The mathematics of the models used is summarized in the Appendix, and the papers cited therein.

This study used physiologically based models to examine the effects of observed weather and projected climate change on several agricultural systems. Historical weather for 105 locations for the period 1995-2005 (UC/IPM Program)[1] was used to develop and test the models and to make predictions of crop-pest-natural enemy interactions given current conditions and assumptions about climate warming. Predicted weather used in the analysis is for climate-warming scenarios based on assumptions about CO_2 levels for the period 1950−2100 generated by two climate change models (see http://meteora.ucsd.edu/cap/cccc_model.html (i.e., scenarios GFDLB1, GFDLA2, PCMB1 and PCMA2; Hayhoe et al. 2004, Maurer 2005, Maurer and Duffy 2005). Projected weather from these scenarios at seven locations in the Central California in a north south transect (Red Bluff, Redding, Davis, Colusa, Fresno, Bakersfield and Brawley in the extreme south) were selected to illustrate the effects of climate warming on olive/olive fly interactions and yellow starthistle dynamics.

---

[1] University of California Statewide Integrated Pest Management Program (http://www.ipm.ucdavis.edu/)

2.0   The Effects of Climate Warming on Crops and Pests

2.1.   Alfalfa/Alfalfa Pests – Weather Effects on Species Dominance

There are roughly 1500 species of arthropod species in alfalfa, but few cause economic damage. A series of exotic pest have invaded alfalfa and have largely been controlled by introduced exotic natural enemies. Among the introduced pests are the pea aphid (*Acyrthosiphon pisum* (symbol **P**)) and blue alfalfa (*A. kondoi* (symbol **B**)) that initially caused great harm to alfalfa production in California (**A**) as they overwhelmed the capacity of native coccinellids (**C**) to control them. Two parasitoids (*Aphidius smithi* (**S**) and *A. ervi* (**E**)) and a fungal pathogen, *Pandora neoaphidis,* were introduced in a biological control effort resulting in successful control across California and neighboring states. The parasitoid *A. smithi* is specific to pea aphid. It is also ten times more susceptible to the fungal pathogen than is the blue aphid. During the normally wet Northern Californian winter, the pathogen causes catastrophic mortality to pea aphid (Pickering and Gutierrez 1991). However, during hot dry period periods, pathogen abundance declines and pea aphid out-competes blue aphid.

Figure 3 shows assembly diagrams[2] for dry and wet winter scenarios respectively (cf. Schreiber and Gutierrez 1998). The directional arrows indicate time and the symbols and the dashed arrows indicate the sequence when the different species entered the system. During dry winters, species A, P, and S dominate (note the larger symbols), but during wet winters species A, B, and E dominate. The key point is that if climate change occurs in this and other systems, it may upset the balance between species in the food webs leading to new webs and in some cases new distributions of species (natural enemies of grape) and increased pest numbers and pest impact (i.e., pink bollworm in cotton, see below).

---

[2] Assembly diagrams depict the sequence of introduction and the outcome of the interactions.

Dry Winter   **Wet winter**

alfalfa   pea aphid

+ pathogen

{ A + P }

A. ervi   A. smithi

{ A + P + S + E }

blue aphid

A = alfalfa

P = pea aphid

B = blue aphid

S = *Aphiduis smithi*

E = *Aphidius ervi*

{A + P + S +B + E}

alfalfa   pea aphid

+ pathogen

{ A + P }

A. ervi   A. smithi

{ A + P + S + E }

blue aphid

{A + P + S + B + E}
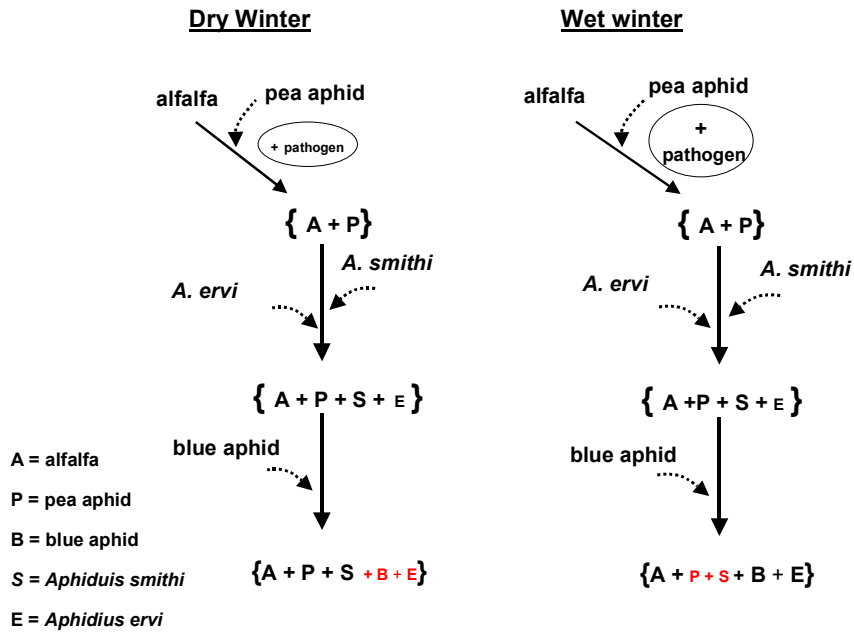
Figure 3. Assembly diagrams (sequence of introduction) for pea and blue aphids and their natural enemies in California alfalfa and the subsequent dominance of different species under dry and wet winters (see text for an explanation).

2.2. Grape/Vine Mealybug

European grape vines are more tolerant of cold than are olives, but temperature could affect not only its productivity but also the quality of the grape and the wine produced from them. This section examines a recent invasive pest of species, the vine mealybug (VMB, *Planococcus ficus*) that has spread throughout much of the grape producing areas of California. Extensive biological control efforts are underway to control this pest, but to date success has been elusive. The introduced natural enemies have different tolerances to temperature (A.P. Gutierrez and K. Daane, 2005 UC/IPM Progress Report). A physiologically based model of grape, VMB and VMB natural enemies was embedded in the GIS and used to assess the effects of recent weather on the control VMB and shows the expected areas where each of the natural enemies would be most effective (**Figure 4**). The major point is that even if successful biological control were to occur, climate change could change all of these interactions and adversely affect control of VMB.
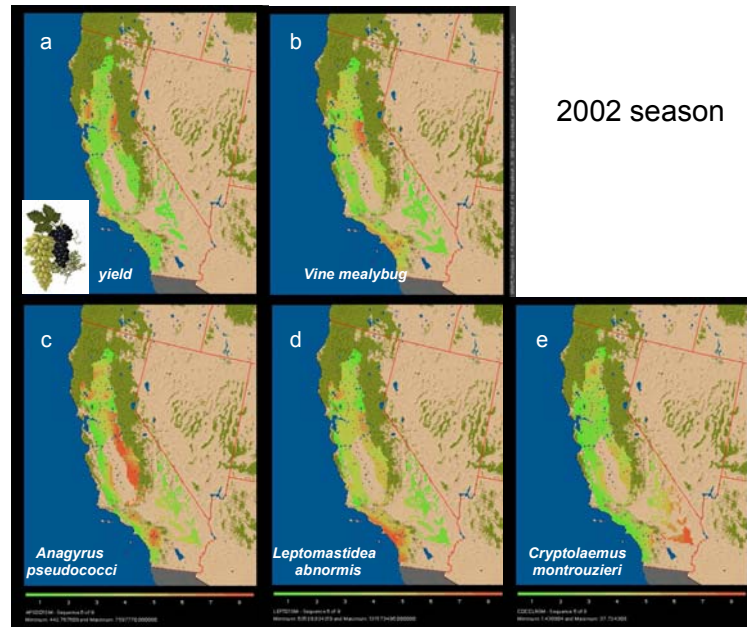
Figure 4. Predicted areas of favorableness for (a.) grape (yield), (b.) cumulative mobile life stages of nine mealybug, (c, d) their parasitism by two of introduced parasitoids (*Anagyrus psuedococci* and *Leptomastidae abnormis*) and (e.) predatory stages of the coccinelid predator *Crytolaemus montrouzieri*. Simulations are for the 2003 season in California Irrigation Management Information System (CIMIS) evapo-transpiration zones 3,5,6,8,10,12,14.

2.3.   Cotton/Pink Bollworm (PBW)

Cotton is grown as an annual in California throughout the southern half of the great Central Valley (i.e., the San Joaquin Valley) and the desert Valleys of southern California favorable climatically and economically for cotton production (see insert in **Figure 5**), but climate warming in California could increase the potential range for cotton production further north into the Sacramento Valley. Here we examine the effects of climate warming on one of its major pests.
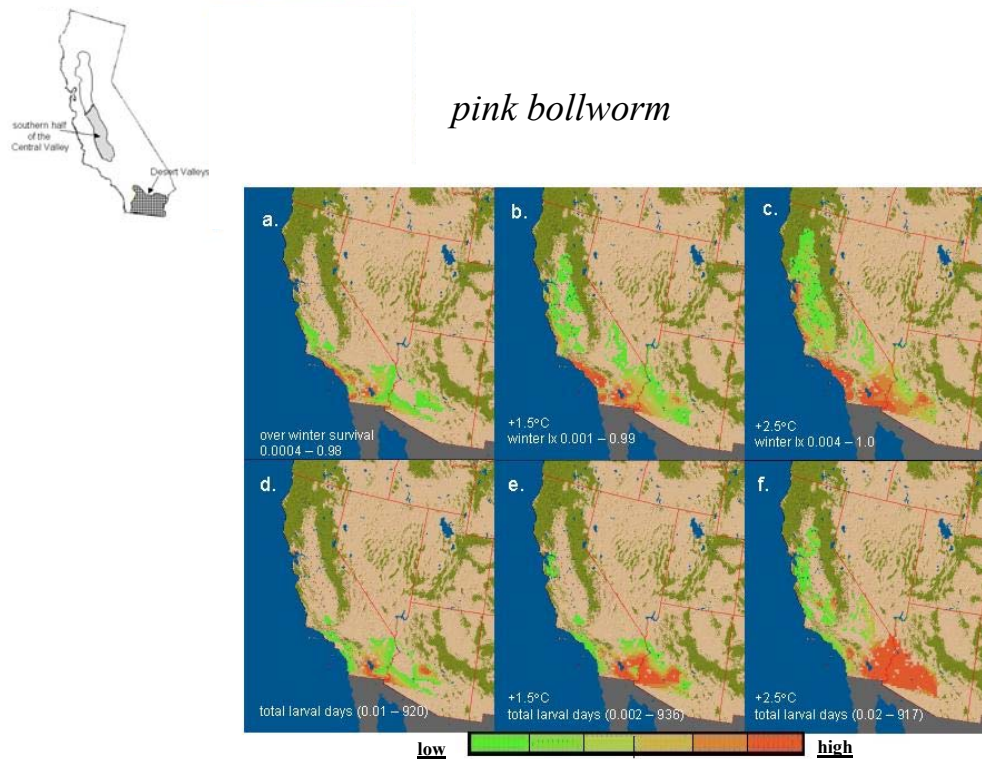
pink bollworm

Figure 5. Cotton/pink bollworm: Predicting areas of favorableness. The effects on winter survival (a-c) and total seasonal pest PBW larval densities (larval days, d-e) under current weather (a, d) and with 1.5ºC (b, e) and 2.5ºC (c, f) increases in daily temperatures respectively (Gutierrez et al. *in press*). The inset indicates where cotton is currently grown.

Pink bollworm (Pectinophora gossypiella, PBW) is a major pest of cotton worldwide, but it geographic range is limited by heavy frosts that kill over-wintering dormant larvae. Using the growth index approach and the commercial software (CLIMEX, see Sutherst et al. 1991), Venette et al. (2000) concluded that abiotic factors did not preclude the establishment of PBW over much of the cotton growing regions of the SE United States. Important limitations of CLIMEX are that it does not include the temporal dynamics and biology of the crop or the pest as driven by weather, and often the only weather data used in the analysis are averages on different time scales (Gutierrez et al. in press). For this reason, a physiologically based model of cotton growth and development and pink bollworm was used that was embedded in a GIS. The model is driven by weather and in a GIS was used to assess the effects of climate warming on the potential distribution of PBW culture in California. Using observed daily weather data, the model predicts, as observed, that PBW is an important pest in California, only in the southern desert valleys (e.g., the Imperial and Coachella valleys and along the Colorado River) (**Figure 5a, d**). Winter frosts restrict PBW's invasion of the million acres of cotton grown in the San Joaquin Valley (e.g., Gutierrez et al. 1977, in press). However, if global warming were to increase winter temperatures, for example, 2ºC-2.5ºC, this warming

8

would greatly increase winter survival and extend the range of this pest northward into the San Joaquin Valley, and furthermore, damage levels would increase in it extant range in the southern desert valleys of California and in Arizona (Gutierrez et al. in press, **Figure 5b,c, e, f**).

2.4. Olive/Olive Fly

Specifically, olive is a drought tolerant long-lived plant which distribution is limited primarily by temperatures. Most temperate climate fruit trees (e.g., pome and stone fruits) as well as olive require winter chilling (i.e., vernalization) to stimulate fruit bud production and blooming (see Hartmann and Opitz 1980). Failure to receive adequate chilling causes failure in fruit buds formation but not vegetative growth as observed in more tropical areas where olive may grow as an ornamental without producing fruit. Mancuso et al. (2002) used artificial neural networks to forecast olive phenology, and DeMelo-Abreu et al. (2004, eqn 1 on page 119) used thermal summing models to estimate flowering dates based on hours chilling requirements for dormancy release and flowering of different varieties of olive. We use average values (e.g., 450h chilling below and 500 degree-days (dd) above a threshold of 7.3°C) in this study of olive production in California.

In addition, freezing temperature may limit olive culture. Denney et al. (1985; see also Dalla Marta et al., 2004) reviewed this literature and proposed a damage index models (I_d, **eqn. 2**, see page 230) for assessing the effects of the frequency of low (and high) temperatures during critical periods on damage to olive and its potential geographic distribution. Cumulative daily damage indices for each year were computed using the four climate change scenarios at seven locations.

$$I_d = f_{SD} + 2f_K + 0.5f_{SF} + 0.25f_{HD} \tag{2}$$

The weights represent the severity of the following effects,

f_{SD} = the number of days with temperature $\leq$ –8.3°C (i.e., light damage),

f_K = days with temperature $\leq$ –12.2°C (killing damage),

f_{SF} = days with $\leq$ 0°C after the beginning of max temperatures $\geq$ 21°C (non killing frost),

f_{HD} = days with temperatures $\geq$ 37.8°C during April or May (during the bloom period).

2.4.1. Olive Model/GIS Mapping

A physiologically based model of olive growth and development was embedded in the GIS and used to assess the effects of climate warming on olive production and potential distribution of olive culture in California. The results for 2003 are summarized in **Figure 6**. Spring frosts can reduce yield and/or freezing temperatures can kill olive trees, which limits the olive's northern range in the Great Central Valley. An arbitrary value of 40 *dd* below 0°C is used to determine when olive tree are killed by frosts. In contrast, lack of "chilling" and high-temperatures during blooming reduces fruit production in some areas (e.g., the southern desert regions of California).
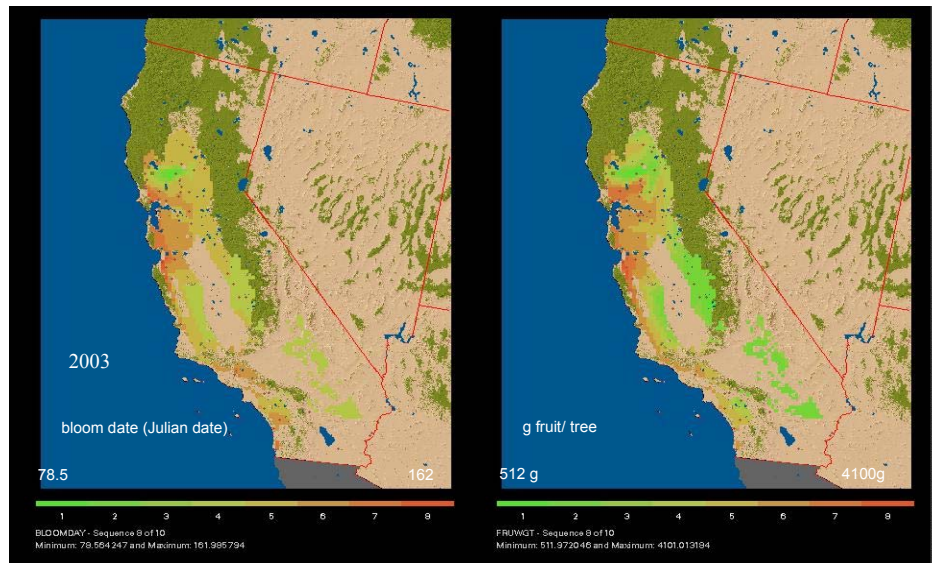
Figure 6. Simulated bloom dates and yield (g/tree) during 2003 in California Irrigation Management Information System (CIMIS) evapo-transpiration zones 3,5,6,8,10,12,14.

The latest bloom dates and highest yield are indicated by red, and the shortest bloom dates and lowest yields are indicated by green. While the predicted distribution of favorableness accords well with areas of olive culture in California, a more detailed analysis is in order.

2.4.2. Simulation of olive growth and development using 150-year projected GFDL weather data.

Model output from Davis, California over 150 years of projected climate change (i.e., the GFDLB1 scenario) shows that season length increases with increasing variability (**Figure 7a**), the frequency of spring frosts deceases (**Figure 7b**), bloom date are earlier (**Figure 7c**), and predicted yields decline even in the absence of olive fly (i.e., with good pest control) as plant respiration increases with temperature (**Figure 7d**). With infestations of the invasive olive fly and in the absence of pest control, yields at Davis are low during the first 120 years and then begin to increase slightly (**7e vs. 7d**) as high temperatures due to global warming become increasingly unfavorable for olive fly (7**f**) (i.e., poor climate matching for the fly).
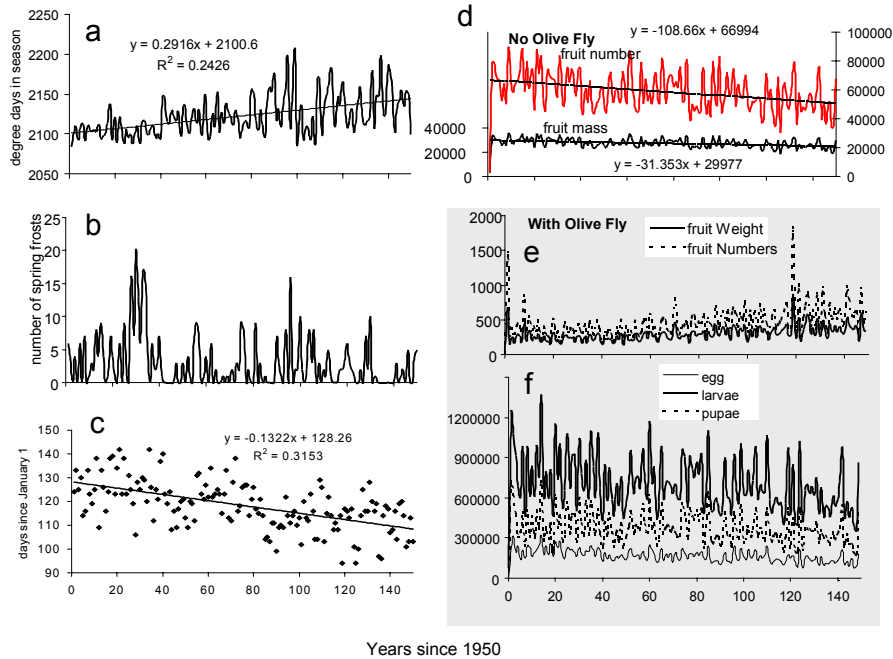
Figure 7. Simulations of olive using 150 years of GFDLB1 projected weather: (a) season length, (b) spring frost days, (c) day to olive bloom, (d) olive fruit number and mass w/out olive fly, as well as with olive fly infestations, (e) olive fruit number and mass with olive fly, and (f) olive fly eggs, larvae and pupae.

Using the GFDLA2 data for projected weather at Davis, California, (**Figure 8a**.), the degree-days during the season increases at a faster rate than in the GFDLB1 scenario, and the number of spring frosts decreases (**Figure 8b**). The tradeoff between these two variables slows the time to bloom date (**Figure 8c**, 0.086 days per year) because the vernalization requirement of olive is delayed. Fruit yield deceases in the absence of olive fly again due to increasing respiration costs (see **Figure 6**). With uncontrolled olive fly infestations (**Figure 8f**), yields are severely depressed (**Figure 8e**) but increase to near normal levels after year 125 (i.e., 2075) but with greatly increased variability. Yield increases are due to decreased favorableness for the more sensitive olive fly due to high temperatures closer to its climatic limits.

11
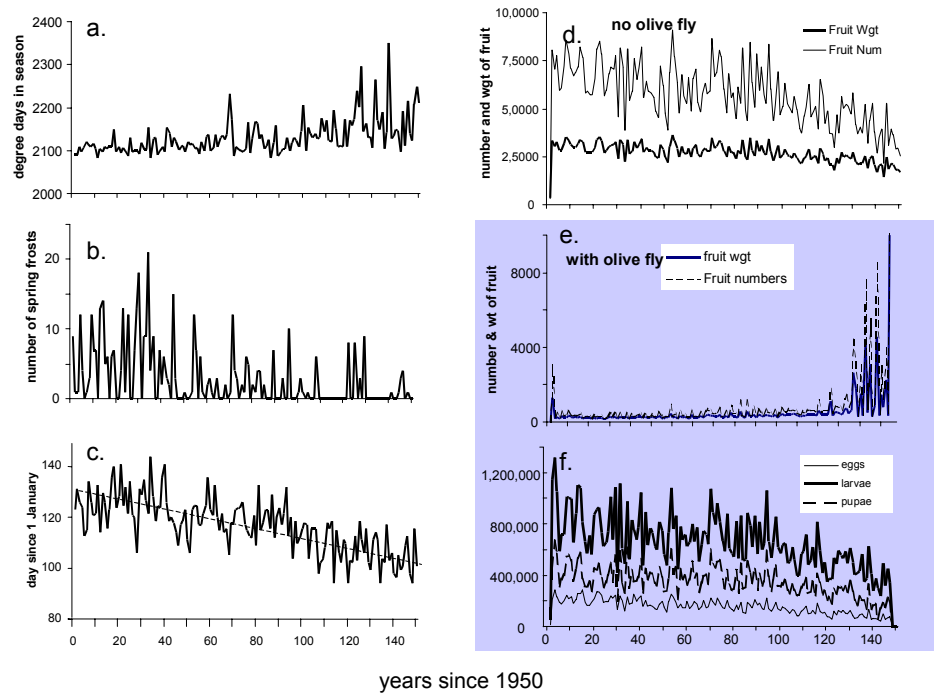
Figure 8. Simulations of olive using 150 years of GFDA2 projected weather: (a) season length, (b) spring frost days, (c) day to olive bloom, (d) olive fruit number and mass w/out olive fly, as well as with olive fly infestations, (e) olive fruit number and mass with olive fly, and (f) olive fly eggs, larvae, and pupae.

2.4.3. Comparing climate change scenarios (PCMB1, PCMA2, GFDLB1, GFDLA2) at seven locations

Seven locations on a north south transect down the middle of the Great Central Valley of California were selected to compare time to bloom and the severity of yearly cumulative temperature damage indices to both low and high temperatures.

PCMB1- Conditions are favorable for olive at all locations except Brawley in the very south of California where vernalization requirements were infrequently met (i.e., the spikes). The cumulative yearly damage index (eqn. 2) due to low or high temperatures is low at Brawley and highest (but highly variable) at Redding, California (**Figure 9**). Similarly, the time to bloom is longer at Redding, declining with decreasing latitude, and being shortest at Bakersfield (day 115 in year 1950 and day 105 in year 2100).

Figure 9. Simulations of olive, using 150 years of PCMB1 projected weather predicting days to olive bloom and cumulative temperature damage index at seven locations (see map insert).

PCMA2 - Conditions are favorable for olive at all locations except Brawley in the very south of California and at Colusa north of Sacramento (**Figure 10**). Vernalization requirements were met infrequently at Brawley (i.e., the spikes, bloom date generally < 100), while predicted killing frosts occurred (i.e., threshold of 40 *dd* below 0°C) at Colusa terminating olive culture there. We note, however, that a subsequent run eliminating the effects of killing frosts shows that in the latter half of the simulation period, warming climate suggests favorableness for olive production (see **Figure 13** below). The cumulative yearly temperature damage indices due to low or high temperatures are lowest at Brawley and highest at Redding, California, and Colusa. The time to bloom is longest at Redding declining with decreasing latitude and being shortest at Bakersfield.
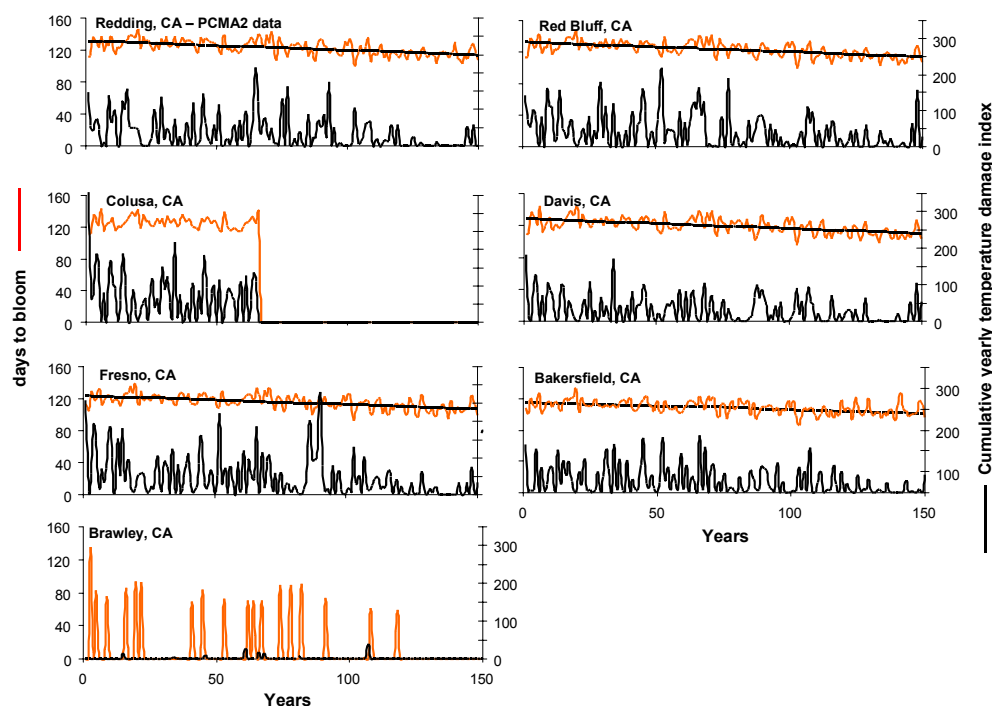
Figure 10. Simulations of olive, using 150 years of PCMA2 projected weather predicting days to bloom and cumulative temperature damage index at seven locations.

GFDLB1 - Using the GFDLB1 projected weather data, conditions are favorable for olive at all locations except Brawley because of unmet vernalization requirements, and Colusa and Red Bluff where heavy killing frosts are predicted (**Figure 11**). Cumulative yearly damage indices are low at Brawley and high at Redding (ca 150), and are extremely high at Colusa (> 300). Olive growth ceased due to killing frosts at Red Bluff and Colusa (see **Figure 13** below). In favorable areas, the time to bloom is longer at Redding, declining with decreasing latitude, and being shortest at Bakersfield.

14
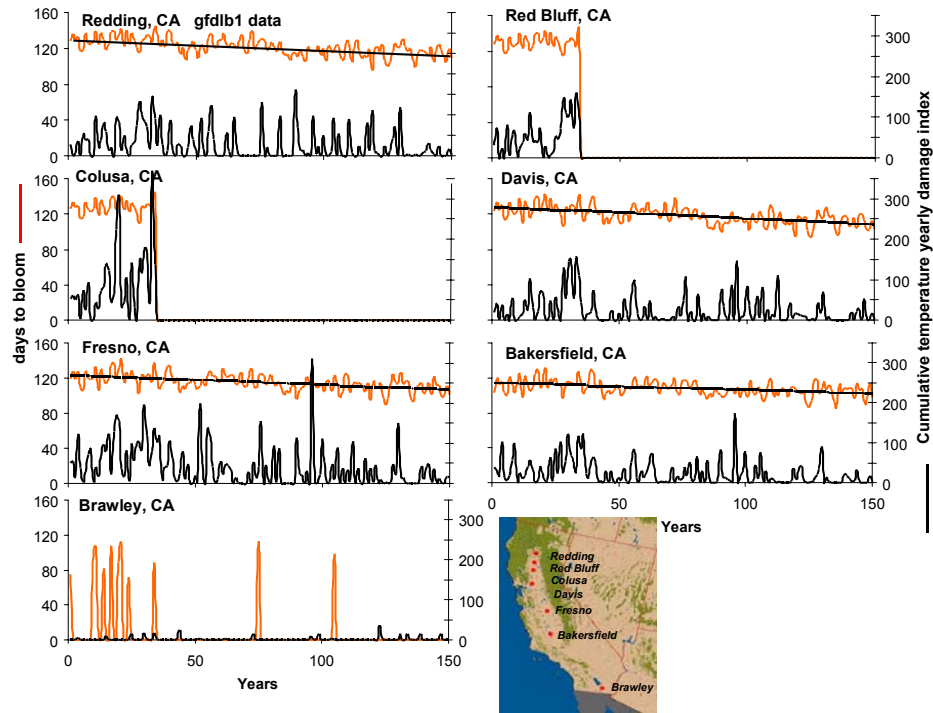
Figure 11. Simulations of olive, using 150 years of GFDLB1 projected weather predicting days to bloom and cumulative temperature damage index at seven locations.

GFDLA2 – Using GFDLA2 weather, conditions are favorable for olives only in the central part of the range (Davis, Fresno, and Bakersfield) and unfavorable in the northern part of the range (Redding, Red Bluff, and Colusa—and at Brawley in the very south of California (**Figure 12**). Vernalization requirement were met infrequently at Brawley, while killing frosts occurred at Redding, Red Bluff, and Redding (40 *dd* below 0°C). As in the other scenarios, climate warming increases favorableness for olive culture during later years of the run. In the locations favorable for olive growth using our freezing criteria, the cumulative yearly damage indices were lowest at Brawley and highest at Davis, California. The time to bloom is longer at Davis declining with decreasing latitude being shortest at Bakersfield.
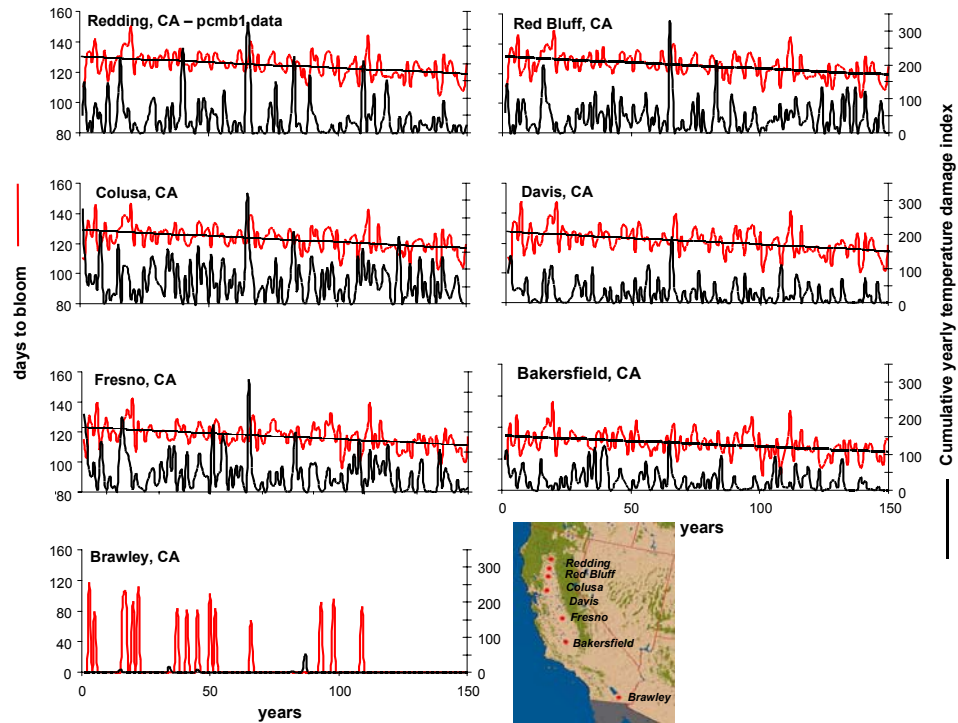
15
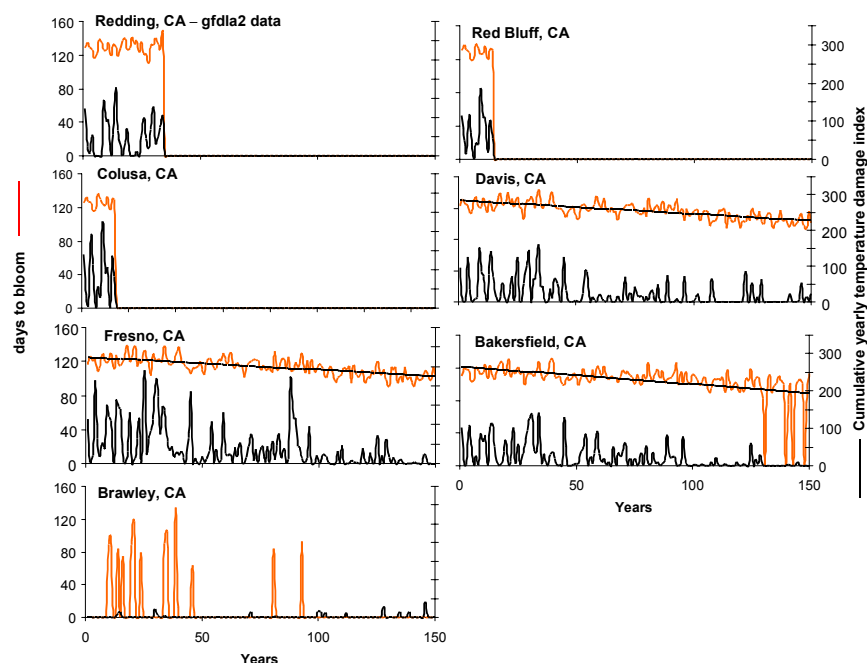
Figure 12. Simulations of olive using 150 years of GFDLA2 projected weather predicting days to bloom and cumulative temperature damage index at seven locations.

2.4.4. Comparison of weather scenarios at Colusa, California, the suppressing the effects of freezing temperatures on olive survival

Suppressing the effects of tree-killing low temperatures in the model, the predictions of the olive models using the four climate warming scenarios for Colusa are compared in **Figure 13**. The goal is to examine whether favorableness for olive culture increases over time in this area. Note that only in the original PCMB1 simulations (**Figure 9**) did the model not predict death of the plant at any of the seven locations. Similar analyses could be performed for other locations and scenarios where the model predicts death of the olive tree due to low temperatures (e.g., Red Bluff and Redding).

The time to bloom declines 0.126 days per year and 0.169 days per year in the GFDLB1 and GFDLA2 scenarios, respectively, and 0.080 days and 0.121 days in the PCMB1 and PCMA2 scenarios. The intercepts among the scenarios are essentially the same. Note that the temperature damage indices in the GFDLB1 and GFDLA2 are initially high but decline over the 150-year simulation run, while values in the PCMB1 and PCMA2 scenarios remain relatively constant.

16
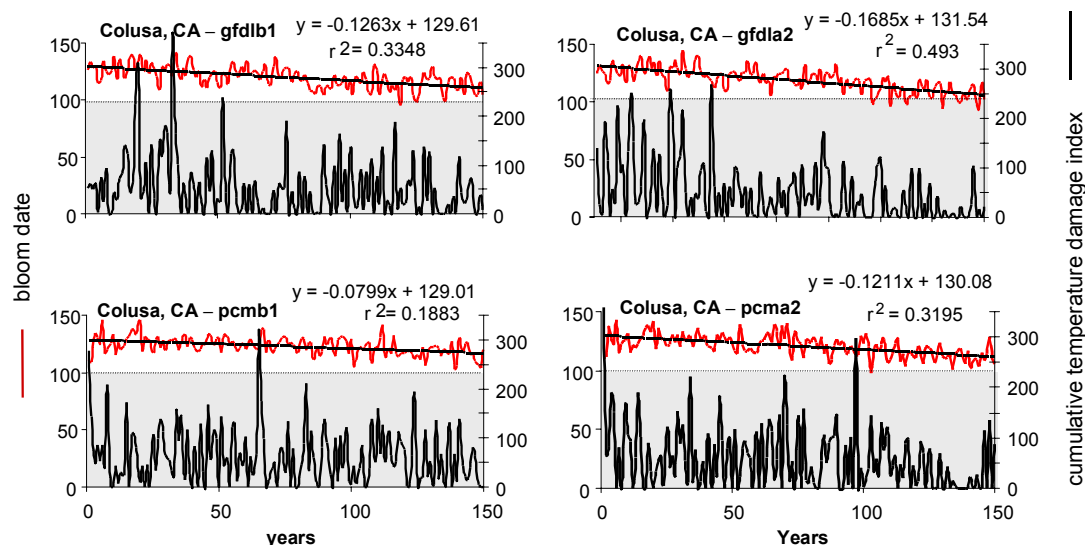
Figure 13. Simulations of olive at Colusa, California, using 150 years of projected weather data for the four scenarios to predict days to bloom and the cumulative temperature damage index (eqn 2).

In summary, the GFDL scenarios are more severe than the PCM scenarios—not because of global warming, but rather because of the effects of low temperatures that decreased olive tree survival during the initial years of the run. The scenario GFDL2a was more severe than the GFDL1B scenario. Climate change across our north-south gradient predicts that more northern areas become more favorable (fewer frosts), while more southern areas become less unfavorable due to decreases in chilling required for vernalization. With global warming, olive production would be consolidated in the central areas of California—the areas of current favorableness.

Climate change would have similar affects on the distribution of the cold intolerant olive fly, as well as other cold intolerant fruit flies such as the Mediterranean fruit fly (*Ceratitis capitata*) which range is currently restricted to more southern climes (Messenger and Flitters 1954). Currently, there are incipient medfly populations in southern California (Carey 1996) with occasional infestations and winter dieback in more northern areas.

2.5. Yellow Starthistle

Many exotic plants have become important weeds in California agriculture, rangelands and waterways. Yellow starthistle (YST, *Centaurea solstitialis*) is an important rangeland weeds in California as it reduces forage quantity and quality, may cause injury to

17

livestock, is a severe nuisance in recreational areas and is highly toxic to horses. Its southern distribution appears to be limited by soil moisture, in the central part of its range in California currently available biological control agents appear to be ineffective. Several natural enemies attacking YST seed heads (capitula) are currently established and include weevils (*Bangasternus orientalis* (*Bo*) and *Eustenopus villosus* (*Ev*) (Coleoptera: Curculionidae)) and two tephritid flies (*Urophora sirunaseva* (*Us*) and *Chaetorellia succinea* (*Cs*) (Diptera: Tephritidae)).
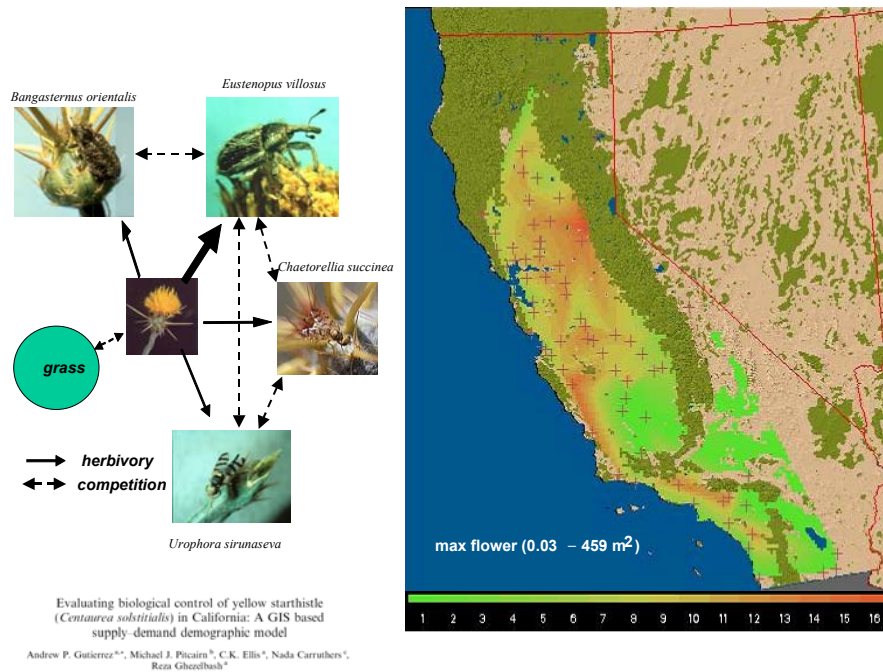
Figure 14. The simulated distribution of yellow starthistle (*Centaurea solstitialis*) flower head densities (capitula) during 2003 in California given the effects for four introduced natural enemies and competition from annual grasses (cf. Gutierrez et al. 2005).

The interactions of the YST-natural enemy system were recently analyzed (Gutierrez et al. 2005). Using multivariate regression to analyze model output across all ecological zones, they were able to assess the role of the major factors in reducing YST abundance. The impact of the natural enemies and competition from grass were included as presence - absence (i.e., 0 or 1) in all possible combinations. Only regression coefficients with slopes significantly different from zero were retained in the model. The runs included all combinations of grass and herbivores.

Using marginal analysis (i.e., dy/dx_i) suggests that the number of capitula m^{-2} increases with season length (*dd* = degree days > 8°C), cumulative rainfall (*mm*), and *Cs* presence, but is greatly reduced by predation by the snout weevil *Eusenopus villosus* (*Ev*) presence with the contribution of the *EvxCs* interaction playing a net minor role.

18

$$capitula = 171.8 + 0.052dd + 0.16mm - 105.3Ev + 22.3Cs -$$
$$29.8Ev \times Cs \tag{3}$$
$$R = 0.53,\ F = 248.6,\ df = 3234$$

Using average values for *dd* and *mm*, average capitula density across the entire region would remain 271m^{-2}.

The regression model of log$_{10}$ seed bank density across all sites on season length (*dd*), total rainfall (*mm*), *E. villosus* and *C. succinea* is eqn 4. Natural enemies *B. orientalis* and *U. sirunaseva* were estimated to occur in very low numbers region wide and, thus, appear to have little effect in reducing seed pool densities and hence were not included in the regional analysis.

$$\log_{10} seed\ density = 3.30 + 0.00007dd + 0.0002mm - 0.18Ev - 0.36Cs + 0.16EvCs$$

$$\tag{4}$$

$$R = 0.42,\ F = 141.4,\ df = 3234$$

Taking the antilog of eqn. 4 and substituting the mean value for *dd* (=2,656) and *mm* (=466) across sites shows that yellow starthistle seed densities increase with season length and total rain fall but decease with *Ev* and *Cs* presence.

$$seed\ density = 10^{3.3}10^{0.00007dd}10^{0.0002mm_{rain}}10^{-0.18Ev}10^{-0.36Cs}10^{0.16EvCs} = 1581\,m^{-2}\qquad,$$
where
$$\begin{cases} 10^{3.3} = 19{,}95 \text{ is a constant.} \\ 10^{0.00007\,dd + 0.0002\,mm} \text{ is the average increase in seed production due to } dd \text{ and rain.} \\ 10^{-0.18\,Ev - 0.36\,Cs + 0.16EvCs} \text{ is net survival rates from seed predation.} \end{cases}$$

The combined action of *E. villosus* and *C. succinea* on average reduce seed production 58% across the entire region with *Cs* having the greatest impact. The impact of *C. succinea* is reduced by its interaction *E. villosus* because the weevil larva kills fly larvae when they co-occur in capitula. The *EvxCs* interaction increases seed survival 12.8% offsetting much of *Ev's* contribution.

Unfortunately, this mortality is insufficient as it allows more than enough seed to survive to maintain high mature plant populations at average densities of 166m^{-2}. The predicted range and abundance of YST in California is shown in **Figure 14**, and accords well with survey data reported by the California Department of Agriculture. In conclusion, YST is the object an intense but so far failed biological control effort introducing seed-head feeding insects. The model suggests that natural enemies that attack the whole plant are likely to be better agents. The effect of climate warming on YST distribution, abundance and the effectiveness of natural enemies control is explored below.

2.5.1. Comparing the four climate warming scenarios on YST abundance

Simulation runs were made for the seven locations included all of the species illustrated in **Figure 14**. The predicted patterns of abundance of germinating YST plants from the soil seed bank are simulated for seven locations using projected GFDLB1 and PCMB1 weather scenarios. All locations had the same initial soil seed bank densities (1500 m^{-2}), but thereafter local production and surviving seed were the conditions for subsequent years (see Gutierrez et al. 2005).

GFDLB1 scenario - YST seedling densities generally increased with increasing latitude becoming extremely abundant in the northern part of the range (**Figure 15**). Densities at Brawley and Bakersfield were low and appear to decrease with time (usually < 25 m^{-2}), while densities at Fresno >100 but were intermittently high, while densities at Davis, Colusa and Red Bluff were usually >200-300 but on occasion exceeded 1000. At Redding, seedling densities were commonly >500 and frequently exceed 1000 m^{-2}. There is a trend of increasing YST abundance with increasing latitude. No increasing trends are seen over time at any of the locations.

Figure 15. Simulation of yellow starthistle including the natural enemies illustrated in Figure 14 using the weather scenario GFDLB1 at seven locations. Seedling density is used as a measure of YST's potential in the area. The reference line at 50 and at 1000 is for comparative purposes.

20

Using the number of mature capitula m^{-2} as a metric of YST and dd, mm and the density of natural enemy larvae as independent variables (i.e., *E* for *Ev*, *U* for *Us*, *C* for *Cs*), multiple regression analysis of the YST data using the GFDLB1 weather scenario yields the following results.

$$capitula = -211.35 + 0.124\,year - 0.0089dd - 0.0924E + 0.027U + 0.041C$$
$$+ 0.000005E \times U - 0.000072E \times C + 0.000006U \times C \qquad (5)$$
$$R^2 = 0.65, \quad df = 1048, \quad F = 244.65$$

Using marginal analysis (i.e., dy/dx_i), the results suggest that seed head densities increased on average 0.124 per year, but decreased 0.0089 per degree-day (*dd*). Of the natural enemies (*total larvae m^{-2}*), only the snout beetle *E. villosus* *(E)* (Coleoptera: Curculionidae) reduced seed head densities while the net effect of the two flies (*Urophora sirunaseva (U)* and *Chaetorellia succinea* (C) (Diptera: Tephritidae)) resulted in a net increase due to competition. Surprisingly, total rainfall during the season was not significant, nor was herbivory from the snout beetle *Bangasternus orientalis*. An additional regression showed that seed head densities also increased with latitude (19 seed heads m^{-2} per degree). Below we explore the PCMB1 scenario, but do not perform a marginal analysis on the data.
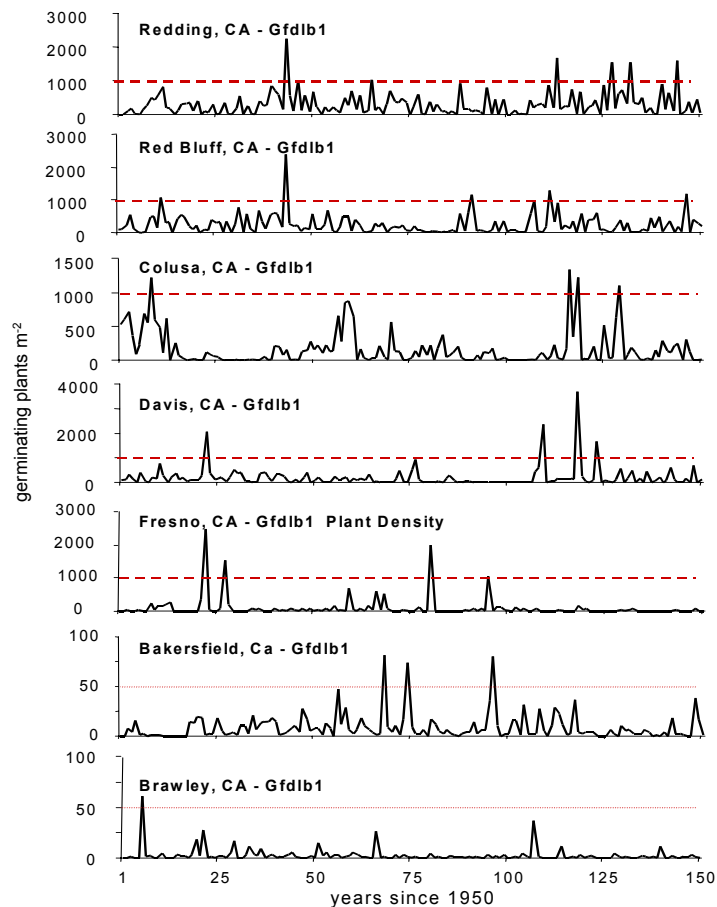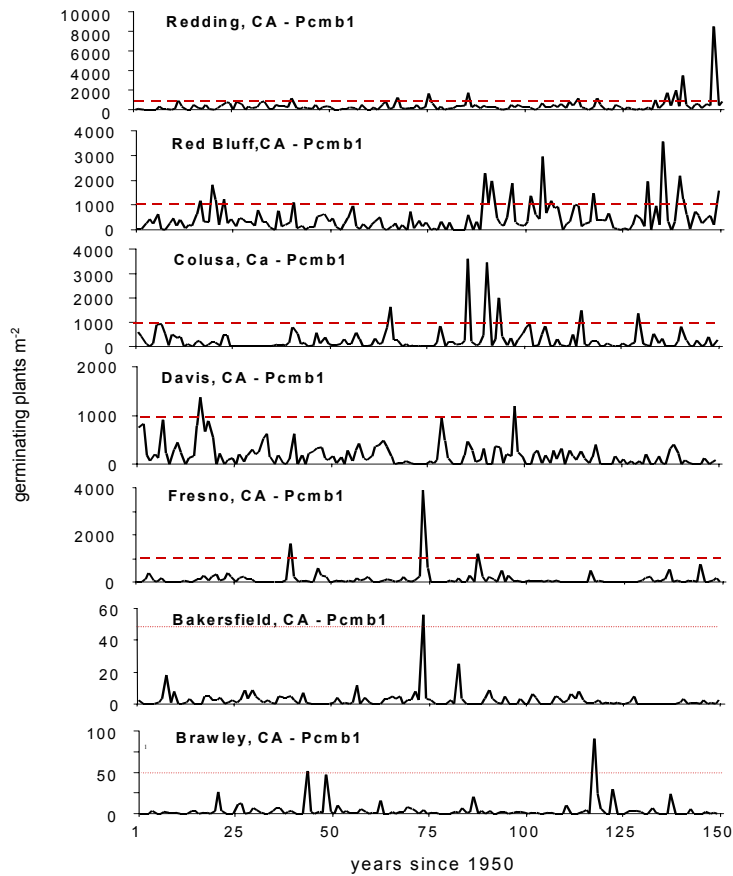
Figure 16. Simulation of yellow starthistle including the natural enemies illustrated in Figure 14 using the weather scenario PCMB1 at seven locations. Seedling density is used as a measure of YST's potential in the area. The reference line at 50 and at 1000 is for comparative purposes.

PCMB1 scenario - In general, YST seedling densities generally were greater in the PCMB1 scenario than in the GFDLB1 scenario, and again seedling densities increased with increasing latitude becoming extremely abundant in the northern part of the range (> 1000 m^{-2} at Redding, **Figure 16)**. Densities at Brawley and Bakersfield were low (usually < 20m^{-2}), while densities at Fresno were > 100, those at Davis and Colusa were >300. Seedling densities were >700 at Red Bluff. In some southern areas, YST seedling densities appear to decrease with time. There is, however, a noticeable increase in YST at Red Bluff after year 85 (roughly 2035) and indications of increases at Redding after year 130 years (roughly 2080).

In summary, YST seedling abundance decreased in the hotter parts of its range and increased in severity northward into formerly colder less favorable areas under both GFDLB1 and PCMB1 climate warming scenarios (**Figures 15 and 16**).

22

3.0   Discussion

That weather is an important factor limiting the potential geographic distribution and abundance of pest and non-pest species is well known. Classic studies of the effects of weather on pest outbreaks is that of locust species in North Africa and the Middle East were they decline to extremely low numbers during periods of drought, but may explode to biblical proportions during prolonged region-wide rainy periods (e.g., Roffey and Popov 1968). Some recent analyses of the effects of weather on pests include Drake (1994), Ellis et al. (1997), Fleming (1996), and Fleming and Candau (1998).

Gutierrez et al. (1974), Gutierrez and Yaninek (1983), Hughes and Maywald (1990) used a growth index approach to determine the weather conditions favorable for establishment and outbreaks fast reproducing aphids in Australia. While this approach worked well for the highly migratory cowpea aphid, it would not likely work as well for long lived pests such as locust across the vast affected areas of North Africa and the Middle East. This is due to the long period of time required for the outbreaks to develop and shifting nature of the problem across the landscape. Physiologically based models capture the effects of weather on the regional dynamics of pests and natural enemies and provide an excellent way to evaluate such complicated systems (Gutierrez 1996; Schreiber and Gutierrez 1998).

The same approach could be used to assess what would happen to the distribution and abundance of crops and pest and non-pest species if temperatures and/or rainfall changed in response to climate change. The model was used to evaluate effect of climate change scenarios on olive culture across the length of California's Great Central Valley. Unlike annual crops that may be easily planted in new areas, long-lived plants such as olive and grape are costly in time and money to reestablish in new locations.

The effects of weather on pests are recurring in most of our examples. One can envision the invasion of new areas by pests formerly limited by one or more constraints. For example, the range of the cotton pest pink bollworm worldwide is limited by winter frost, hence the predicted milder winters would increase its range northward, say into the San Joaquin Valley of California. The cotton boll weevil is limited by desiccation of fruit buds in hot dry areas (DeMichele *et al*. 1976); hence if summer rainfall increased, its geographic range within California might also increase. This expansion of range and abundance occurred during the early 1980s when a sequence of very wet years in Arizona and Southern California coupled with the cultivation of stub-cotton temporarily increased the threat from boll weevil. The threat subsided as drier weather returned. How many other pest species will be similarly affected is at present unknown, and will require analysis. Would pest population outbreaks be more frequent and more prolonged as is the case for pink bollworm?

Similarly, climate change would simply complicate the problem of pest regulation by natural enemies (i.e., biological control). Examples abound in the literature and several examples in such diverse crops as alfalfa, citrus, grape, and the weed yellow starthistle (YST) were discussed. In YST, control by plant feeding natural enemies has been checkered because each of the introduced herbivore natural enemies causes it own type of damage and each has it own climatic requirements that limit its geographic range of

maximum effectiveness. In general, control of YST has been poor throughout California because the natural enemies have a negative density dependent relationship with the flower heads they attack and only partial destruction of the seed in them occurs. This is confirmed by our analysis. Better biological control has been reported in Oregon where the shorter growing season reduces YST's capacity to compensate for herbivore damage, but this could change with climate warming. An analysis by Gutierrez et al. (2005) suggests that natural enemies that attack the whole plant and reduce its capacity to produce seed and to compensate for competition and damage would be better candidates for introduction, but even these species would be affected by climate change in unknown ways. Examples of such natural enemies are a pathogenic fungus specific to YST is being released in California, and a host-specific insect species that damages the root system is being evaluated for introduction (United States Department of Agriculture (USDA)/Albany, California, and the California Department of Food and Agriculture (CDFA)). Because of the tremendous losses accruing to California agriculture from exotic insect pests and weeds, additional support for biological control would appear to be warranted and highly cost effective.

Assessing the impact of climate warming on crop pest-natural enemy interactions is difficult and requires simplified but realistic models to examine these issues. The current limitation to implementing a physiologically based modeling approach is the lack of infrastructure for developing the models and for collecting the requisite biological and weather data to implement them. There are also large gaps in the development and refinement of such models and the availability of appropriate weather data to implement them and to project model results on a large geographic scale. The cost to correct these deficiencies is relatively small, while the potential benefits are large. The development of such system models for the major crops in California was a major goal, now abandoned, of the UC/IPM Statewide Program when it was first started in 1978.

4.0   References

Bieri, M., J. Baumgärtner, G. Bianchi, V. Delucchi & R., Von Arx. 1983. Development and fecundity of pea aphid (*Acyrthosiphon pisum* Harris) as affected by constant temperatures and pea varieties. Mitt. Schweiz. Entomol. Ges. 56:163-171.

Campbell, A., B. D. Frazer, N. Gilbert, A. P. Gutierrez and M. Mackauer. 1974. Temperature requirements of some aphids and their parasites. J. Appl. Ecol. 11: 431-438.

Carey, J.R. 1996. The incipient Mediterranean fruit fly population in California: implications for invasion biology. *Ecology* **77** (1996), pp. 1690–1697.

Dalla Marta, A., S. Orlandini, P. Sacchetti and A. Belcari. 2004. *Olea europaea*: integration of GIS and simulation modeling to define a map of "dacic attack risk" in Tuscany. Adv. Hort. Sci. 18(4):168-172.

DeBach, P. 1964. *Biological control of Insect Pests and Weeds*. Chapman and Hall, London, pp. 844.

DeBach, P. and R.A. Sundby. 1963. Competitive displacement between ecological homologues. Hilgardia 34:105-166.

DiCola, G., G. Gilioli & J. Baumgärtner. 1999. Mathematical models for age-structured population dynamics. In *Ecological Entomology*, (C. B. Huffaker and A.P. Gutierrez, editors, second edition) John Wiley and Sons. New York. Pp.503-534.

DeMelo-Abreu, D. Barranco, A.M. Cordiero,, J. Tous, B.M. Rogado and F.J. Villalobos, 2004. Modelling olive flowering date using chilling for dormancy release and thermal time. Agric. For. Meteorology 125:117-127.

DeMichele, D.W., G.L. Curry, P.J.H. Sharpe and C.S. Barfield. 1976. Cotton bud drying: A theoretical model. Environ. Entomol. 5:1011 - 1016.

Denney, J.O. and G.R. McEachern, 1985. Modeling the thermal adaptability of the olive (*Olea europaea* L.) in Texas. Agric. For. Meteorology, 35:309-327.

Drake, V A. 1994. The influence of weather and climate on agriculturally important insects: An Australian perspective. Aust. J. Agric. Res. 45: 487-509.

Ellis, W N, J.H. Donner, and J H. Kuchlein. 1997. Recent shifts in phenology of Microlepidoptera, related to climatic change Lepidoptera). Entomol. Berichten (Amsterdam) 57: 66-72.

Fleming, R A. 1996. A mechanistic perspective of possible influences of climate change on defoliating insects in North America's boreal forests. Silva Fennica, 30: 281-294.

Fleming, R A and J-N. Candau. 1998. Influences of climatic change on some ecological processes of an insect outbreak system in Canada'a boreal forests and the implications for biodiversity. Environ. Monitoring and Assessment 49: 235-249.

Fitzpatrick, E. A. and H. A. Nix. 1970. The climatic factor in Australian grasslands ecology. *Australian Grasslands* (Ed. R. M. Moore). pp 3-26. Australian National University Press.

Gilbert, N. E. and A. P. Gutierrez. 1973. A plant-aphid-parasite relationship. J. Anim. Ecol. (42): 323-340.

Gilbert, N., A. P. Gutierrez, B. D. Frazer and R. E. Jones. 1976. *Ecological Relationships*. Freeman and Co., New York.

Gutierrez, A. P. 1992. The physiological basis of ratio dependent theory. Ecology 73: 1552-63.

Gutierrez, A. P. 1996. *Applied Population Ecology: a supply-demand approach*. John Wiley and Sons, New York. 300 pp.

Gutierrez, A. P., 2001. Climate Change: Effects on Pest Dynamics. In *Climate Change and Global Crop Productivity*, K.R. Reddy and H.F. Hodges editors. CAB International, London.

Gutierrez, A. P. and J. U. Baumgärtner. 1984a. Multitrophic level models of predator-prey-energetics: I. Age specific energetics models-pea aphid *Acyrthosiphon pisum* (Harris) (Homoptera: Aphididae) as an example. Can. Ent. 116: 924-932.

Gutierrez, A. P., Butler, G.D. Jr., Wang, Y., Westphal, D., 1977. The interaction of the pink bollworm, cotton and weather. Can. Entomol. 109: 1457-1468.

Gutierrez, A.P., Ellis, C.K., Ghezelbash, R.. Climatic limits of pink bollworm in Arizona and California: effects of climate warming (submitted) Acta Oecologica **(in press)**

Gutierrez, A. P., L. A. Falcon, W. B. Loew, P. Leipzig and R. van den Bosch. 1975. An analysis of cotton production in California: A model for Acala cotton and the efficiency of defoliators on its yields. Env. Ent. 4(1): 125-136.

Gutierrez, A. P., D. E. Havenstein, H. A. Nix and P. A. Moore. 1974. The ecology of *Aphis craccivora* Koch and subterranean clover stunt virus. III. A regional perspective of the phenology and migration of the cowpea aphid. J. Appl. Ecol. 11: 21-35.

Gutierrez, A. P., S. J. Mills, S. J. Schreiber and C. K. Ellis 1994. A physiologically based tritrophic perspective on bottom up - top down regulation of populations. Ecology 75: 2227-2242.

Gutierrez, A. P., P. Neuenschwander, F. Schulthess, H. R. Herren, J. U. Baumgärtner, B. Wermelinger, J. S. Yaninek and C. K. Ellis. 1988b. Analysis of biological control of cassava pests in Africa: II. Cassava mealybug, *Phenacoccus manihoti*. J. Appl. Ecol. 25: 921-940.

Gutierrez, A.P., Pitcairn, M.J., Ellis, C.K., Carruthers, N., Ghezelbash, R., 2005. Evaluating biological control of yellow starthistle (*Centaurea solstitialis*) in California: A GIS based supply–demand demographic model. Biological Control 34: 115-131.

Gutierrez, A. P. and J. S. Yaninek. 1983. Responses to weather of eight aphid species commonly found in pastures in southeastern Australia. Can. Ent. 115: 1359-1364.

Gutierrez, A. P., B. Wermelinger, F. Schulthess, J. U. Baumgärtner, H. R. Herren, C. K. Ellis and J. S. Yaninek. 1988a. Analysis of biological control of cassava pests in Africa: I. Simulation of carbon nitrogen and water dynamics in cassava. J. Appl. Ecol. 25: 901-920.

Hartmann, H.T. and K.W. Opitz, 1980. Olive production in California, rev. ed. Leaflet 2474, University of California Div. Agric. Sci., Davis.

Hayhoe, K., D. Cayan, C. Field, P. Frumhoff, E. Maurer, N. Miller, S. Moser, S. Schneider, K. Cahill, E. Cleland, L. Dale, R. Drapek, R. M. Hanemann, L. Kalkstein, J. Lenihan, C. Lunch, R. Neilson, S. Sheridan, and J. Verville, 2004, Emissions pathways, climate change, and impacts on California, Proceedings of the National Academy of Sciences (PNAS) 101 (34), 12422-12427.

Hughes, R. D. and G.W. Maywald. 1990. Forecasting the favorableness of the Australian environment for the Russian wheat aphid, *Diuraphis noxia* (Homoptera: Aphididae), and its potential impact on Australian wheat yields. Bull. Entomol. Res. 80: 165-175.

Liebig, von J. 1840. *Chemistry and its Applications to Agriculture and Physiology*. London, Taylor and Walton. (4th edition 1847).

Mancuso, S., G. Pasquili and P. Fiorino, 2002. Phenology modelling and forecasting in olive (*Olea europaea* L.) using artificial neural networks. Adv. Hort. Sci. 16(3-4):155-164.

Maurer, E.P., 2005, Uncertainty in hydrologic impacts of climate change in the Sierra Nevada Mountains, California under two emissions scenarios, Climatic Change (submitted 29 April 2005).

Maurer, E.P. and P.B. Duffy, 2005, Uncertainty in projections of stream flow changes due to climate change in California, Geophys. Res. Let. 32(3), L03704 doi:10.1029/2004GL021462.

Hayhoe, K., D. Cayan, C. Field, P. Frumhoff, E. Maurer, N. Miller, S. Moser, S. Schneider, K. Cahill, E. Cleland, L. Dale, R. Drapek, R. M. Hanemann, L. Kalkstein, J. Lenihan, C. Lunch, R. Neilson, S. Sheridan, and J. Verville, 2004, Emissions pathways, climate change, and impacts on California, PNAS 101 (34), 12422-12427.

Messenger, P. S. 1964. Use of life-tables in a bioclimatic study of an experimental aphid-braconid wasp host-parasite system. Ecology 45: 119-131.

Messenger, P. S. 1968. Bioclimatic studies of the aphid parasite *Praon exsoletum*. 1. effects of temperature on the functional response of females to varying host densities. Can. Ent. 100: 728-741.

Messenger, P.S. and N.E. Flitters 1954. Bioclimatic studies of three species of fruit flies in Hawaii. J. Econ. Entomol. 47:756-765.

Nechols, J. R., M. J. Tauber, C. A. Tauber, and S. Masaki. 1998. Adaptations to Hazardous Seasonal Conditions: Dormancy, Migration, and Polyphenism . In *Ecological Entomology*, C.B. Huffaker and A.P. Gutierrez (eds.), John Wiley and Sons, New York.

Pickering, J. and A. P. Gutierrez. 1991. Differential impact of the pathogen *Pandora neoaphidis* (R. & H.) Humber (Zygomycetes: Entomophthorales) on the species composition of *Acyrthosiphon* aphids in alfalfa. Can. Ent. 123: 315-320.

Pimentel, D., L. Lach, R. Zunig and D. Morrison. 2000. Environmental and economic costs of nonindigenous species in the United States. BioScience 50: 53-65.

Quezada, J.R. and P. DeBach 1973. Bioecological and population studies of the cottony scale, *Icerya purchasi* Mask., and its natural enemies. *Rodolia cardinalis* Mul. And *Cryptochaetum iceryae* Wil., in southern California. Hilgardia 41:631-688.

Reddy, K.R. and H.F. Hodges (editors). 2001. *Climate Change and Global Crop Productivity*,. CAB International, London.

Rochat, J. and A. P. Gutierrez (2001) Weather mediated regulation of olive scale by two parasitoids. J. Anim. Ecol. 70: 476-490.

Roffey J. and G. Popov. 1968. Environmental and behavioural processes in Desert locust outbreaks. Nature 219: 446-450.

Schreiber, S. and A. P. Gutierrez. 1998. A supply-demand perspective of species invasions and coexistence: applications to biological control. Ecol. Modelling 106: 27-45.

Shelford, V. E. 1931. Some concepts of bioecology. Ecology 12: 455-467.

Sutherst, R. W., G. F. Maywald and W. Bottomly. 1991. From CLIMEX to PESKY, a generic expert system for risk assessment. *EPPO Bulletin* 21: 595-608.

Vansickle, J. 1977. Attrition in distributed delay models. *IEEE Trans. Sys., Man. Cybern*. 7: 635-638.

Venette, R.C., Naranjo, S.E., Hutchison, W.D., 2000. Implications of larval mortality at low temperatures and high soil moistures for establishment of pink bollworm (Lepidoptera: Gelechiidae) in Southeastern United States cotton. Environ. Entomol. 29(5): 1018–1026.

Watt, K.E.F. 1959. A mathematical model for the effects of densities of attacked and attacking species on the number attacked. Can. Entomol. 91: 129-144.

Wit de, C. T., and J. Goudriaan, 1978. *Simulation of Ecological Processes* 2nd edit. PUDOC Publishers, The Netherlands.

Appendix

A weather driven tritrophic model

A plant-herbivore (and higher tropic levels) model may be viewed as *ns* {*n* = 1, ns} linked *functional* age/mass structured population models. The plant is a canopy model consisting of five linked demographic models: mass of leaves {*n* = 1}, stem {2} and root {3}, and for fruit mass and numbers {4, 5}.[3] These models {1-5} are linked by photosynthate production and allocation with the ratio of production to demand controlling all vital rates (*cf.* Gutierrez et al. 1988a,b). The age structured number dynamics of herbivore is modeled using a similar model {6} linked to plant fruit models {4, 5} that it uses as hosts for its progeny.

Each of the *functional* populations may be modeled using a time-invariant distributed-maturation time age-structure model (eqn. A1, Vansickle 1977, see DiCola et al. 1999 for related model forms). We use the notation of DiCola et al. (1999, p 523-524) to describe the Vansickle (1977) distributed maturation time model used in our analysis. This model is characterized by assumption

$$v_i(t) = v(t) = \frac{k}{del(t)} \Delta a \qquad i=0,1, \ldots, k \tag{A1.1}$$

where k is the number of age intervals, *del(t)* is the expected value of emergence time and Δa is an increment in age. From (A1.1) we obtain

$$\frac{dN_i}{dt} = \frac{k}{del(t)} [N_{i-1}(t) - N_i(t)] - \mu_i(t)N_i(t) \tag{A1.2}$$

where N_i is the density in the *i*th cohort and $\mu_i(t)$ is the proportional net loss rate. In terms of flux $r_i(t) = N_i(t)v_i(t)$, yields

$$\frac{d}{dt}\left[\frac{del(t)}{k} r_i(t)\right] = r_{i-1}(t) - r_i(t)] - \frac{del(t)}{k} \mu_i(t)r_i(t). \tag{A1.3}$$

The model is implemented in discrete form (see Gutierrez 1996).

---

[3] Brackets {} are used to denote functional ppulation only and not equations which are denoted by ( ).

Aging occurs via flow rates $r_{i-1}(t)$ from N_{i-1} to N_i, births enter the first age class of the population, deaths at maximum age exit the last or kth age class, and net age-specific proportional mortality (losses and gains) from all factors is included in $-\infty < \mu_i(t) < +\infty$. The mean developmental time of a population is v with variance V with the age width of an age class being v/k and $k = v^2/V$. The number of individuals (or mass units) in age class i is $N_i(t) = r_i(t)v \Big/ k$, and that in the total population is $N(t) = \sum_{i=1}^{k} N_i(t) = \dfrac{v(t)}{k} \sum_{i=1}^{k} r_i(t)$. If k is small, the variability of developmental times is large and *vice-versa*. A value of $k = 45$ was chosen to produce a roughly normal distribution of developmental times.

The developmental time of herbivore larvae varies with fruit host age, and both the host and the larvae age on their own temperature-time scale (see below). Hence larvae initially infesting specific age fruits at time t will in the course of their development experience changing host characteristics that affect their developmental times, mortality and potential fecundity as an adult. To handle this biology, a two-dimensional time-invariant distributed maturation time model with flows in the fruit age and age of pest dimensions is utilized (eqn. A2).

$$\frac{dN_{i,j}}{dt} = \frac{k}{del(t)}[N_{i-1,j-1}(t) - N_{i,j}(t)] - \mu_{i,j}(t)N_{i,j}(t) \tag{A2}$$

The mean developmental rate of a cohort of larvae ($v(t,i,j)$) is transient and depends on host fruit age. Hence, if i is larval age and j is its host fruit age, the model is updated for flow first in the ith and then the jth dimension taking care to correct for differences in developmental time scales between cells. For convenience, the net proportional mortality term $\mu_{nij}(t)N_{i,j}$ is applied in the ith dimension and assumed zero in the jth dimension. This scheme also allows mortality to herbivore eggs and larvae due to fruit subunit shedding to be applied to larvae in each i,j cohort. herbivore population density is

$$N(t) = \sum_{j=1}^{k}\sum_{i=1}^{k} N_{nij}(t) = \sum_{j=1}^{k} \frac{v(t,j)}{k} \sum_{i=1}^{k} r_{nij}(t). \tag{A3}$$

Physiological time and age

Plant and its pests are poikilotherms and hence time and age in the model are in physiological time units. The linear degree-day model (A4) was used to model the temperature (T) dependent development rate ($\Delta v(t(T))$) because sufficient data across the full range of temperatures was unavailable.

$$\Delta v(t(T)) = \frac{1}{v(t(T))} = c_1 + c_2 T(t) \tag{A4}$$

Constants c_1 and c_2 are fitted to species data. The lower developmental threshold ($\Delta v(t(T)) = 0$) for the plant and herbivore (and higher trophic levels) may differ. A time step in the model is a day of varying physiological time (degree days d^{-1} = Δdd) computed above appropriate threshold using the half sine method (Gilbert and Gutierrez 1973; Campbell et al. 1974).

Growth rates

As rates, per capita resource acquisition ($S(u)$) is allocated in priority order to egestion (β) respiration (i.e., Q_{10}), costs of conversion (λ) and to reproductive and growth rates (GR).

$$GR(t) = \phi * (t)(S(u)\beta - Q_{10})\lambda \tag{A5.1}$$

The realized *GR* must also include the effects of other limiting factors. This is done by the scalar (ϕ^*) that is the product of the daily supply-demand ratios for the other essential resources (see eqn. 1 and below). Resource acquisition $S(u)$) involves search and depends on the organism's maximum assimilative capacity (i.e., its demand, $D(u)$). This quantity may be estimated experimentally under conditions of non-limiting resource.

$$D(u) \approx S(U) = (GR_{\max}(t)/\lambda + Q_{10})/\beta . \tag{A(5.2)}$$

Resource acquisition - Plants capture light, water and inorganic nutrients and herbivore larvae attack plant subunits (e.g., fruit). The biology of resource acquisition by a

population of plant or animal consumers ($N(t)$) involves search under conditions of time varying resource ($R(t)$). The maximal population demand is $D=D(u)N$. Resource acquisition (S) is modeled using the ratio-dependent Gutierrez and Baumgärtner (1984) functional response model (eqn. A6, Gutierrez, 1992) that is a special case of Watt's model (1959) because it include eqn 5.2 (see Gutierrez 1996 (p. 81) for the derivation of this model). We simplify the notation as follows.

$$S = Dh(u) = D\left[1 - \exp\left(\frac{-\alpha R}{D}\right)\right]. \tag{A6}$$

$h(u)$ is the proportion of the resource demanded (D, eqn. 5.2) obtained and α is the search parameter. α may also be a convex function of N making (A6) a type III functional response (Rochat and Gutierrez, 2001; (i.e., $\alpha = 1 - \exp(-sN)$) with search constant s)). As a function of N, α for plants becomes Beer's Law and for animals it is the Nicholson-Bailey model. Note that intra-specific competition enters the model via the ratio of available resource to population demand ($\frac{-\alpha R}{D}$). Note also that inter-specific competition also enters in this manner.

The resource (R) for plant is the light energy (cal m^{-2}d^{-1}) per unit of ground at time t multiplied by a constant that converts it to g dry matter m^{-2}d^{-1}. For herbivore, R may be the sum of all age fruit (or leaves, age=j) corrected for preference ($0 \le \xi_j \le 1$).

$$R = \sum_{j=1}^{J} \xi_j R_j \tag{A7}$$

Note that stages with preference values equal zero are effectively removed from the calculations.

The total age specific consumer demand (D) across ages ($i= 1, k$) may be computed in mass or number units as appropriate for the population.

$$D = \sum_{i=1}^{k} D_i^* N_i \tag{A8}$$

In plant, the demand rate (g dry matter d^{-1}) is the sum of all subunit population maximum demands corrected the costs of conversion of resource to self and respiration (eqn A5.2, see Gutierrez and Baumgartner, 1984).

In pests such as herbivore, the demand rate is the maximum per capita adult demand for oviposition sites is computed using eqn. A9.

$$D^*_{i=a} = \theta\phi_T(T)f(a) \tag{A9}$$

$f(a) = \dfrac{ca}{d^a}$ is the maximum age (a) specific per capita fecundity at the optimum temperature with parameters c and d (cf. Bieri et al., 1983).

$\theta = 0.5$ is the sex ratio.

$\phi_T(T)$ is the correction for the effect of temperature dependent respiration.

Supply-demand effects - Consumer resource acquisition success is estimated by the acquisition supply/demand ratio ($\phi_{S/D}(t)$) obtained by dividing both side of eqn. A6 by the population demand D.

$$0 \le \phi_{S/D}(t) = S\big/D = h(u) < 1. \tag{A10}$$

Some consumers may have multiple resources and they must be included in the computation (see below).

In plant, success in meeting its demand is measured by the photosynthate *supply/demand* ratio (e.g., $0 \le \phi_{cot,S/D} < 1$) but there may be shortfalls of water (*w*) and inorganic nutrients (η) that may also computed using variants of (eqn. A6). For example, the water $0 \le \phi_w = S_w/D_w < 1$ ratio is computed in three steps: (i) the potential evapo-transpiration ($D_w = PET$) and evaporation from the soil surface (*ES*) are estimated using a Penman based biophysical model; (ii) D_w along with available soil water in the root zone ($w = W_{max} - W_{wp}$) above the wilting point (w_{wp}) are substituted in eqn. A6 to compute evapo-transpiration ($S_w = ET$, i.e., water use by the plant); and (iii) the input-output model balances rainfall (*rain, ES, ET*) and runoff or flow through above maximum soil water holding capacity (W_{max}) (see Gutierrez et al., 1988).

$$w_{WP} \le w(t+1) = w(t) + rain(t) - ES(t) - ET(t) \le W_{max} \qquad (A11)$$

Similarly for nitrogen, $0 \le \phi_\eta = S_\eta / D_\eta < 1$ is computed using analogues of eqns. A6-A 8 and A10 (see Gutierrez et al., 1991b for details).

The combined effect of shortfall of all essential resources is captured as the product of the independent supply-demand ratios (eqn. A12) (i.e., survivorship terms, Gutierrez et al., 1994).

$$0 \le \phi^* = \phi_{(S/D)} \phi_{(w)} \phi_{(\eta)} ... < 1. \qquad (A12)$$

Eqn. A12 is functionally Liebig's Law of the Minimum because if any component of ϕ^* causes the supply to fall below a limiting value (e.g., respiration in plant, see A6), it becomes the limiting factor. In plants, after respiration and conversion costs have been subtracted from $\phi^* D$, the remaining photosynthate is allocated in priority order to meet demands for reproduction and then vegetative growth and reserves (see Gutierrez, 1992, 1996). In addition to slowing the growth rates of subunits, ϕ^* also reduces the production rate of new subunits, the survival of extant ones (e.g., fruit shedding), and in the extreme may causes the death of the whole plants.

Say individual herbivore larvae infest individual fruit making their behavior more akin to that of a parasitoid. For this reason, the effects of temperature on respiration and hence fecundity are introduced in an approximate way. In poikilotherms, respiration increases with temperature and a plot of the net assimilation rate (supply – respiration) on temperature typically yields a humped or concave function over the range favorable for development with zero values occurring at the lower and upper thermal thresholds and the maximum assimilation rate occurs at T_{opt}.[4] This function arises naturally in the plant model. However, to capture the effect of temperature on herbivore fecundity, we assume that the normalized effect of temperature on fecundity (i.e., the physiological

---

[4] This function is similar to the temperatureindex used in CLIMEX, but here the function is applied daily.

index for temperature, $0 \leq \phi_T(t) \leq 1$) is similarly convex (see Gutierrez et al., 1994, Rochat and Gutierrez, 2001). The simplest form for ϕ_T is convex symmetrical (eqn. A13).

$$\phi_T = \begin{cases} 1 - \left(\dfrac{(T - T_{min}) - \gamma}{\gamma} \right)^2 & \text{if } T_{min} \leq T \leq T_{max} \\ \text{otherwise} \quad 0 \end{cases} \tag{A13}$$

The temperature thresholds for development are T_{min} and T_{max}, and $\gamma = T_{max} - T_{min})/2$ is half the favorable range and $T_{opt} = (T_{max} + T_{min})/2$ is the midpoint.